Pure Component and Binary Vapor−Liquid Equilibrium + Modeling for Hexafluoropropylene and Hexafluoropropylene Oxide with Toluene and Hexafluoroethane

Shalendra C. Subramoney,[†] Wayne M. Nelson,[†] Alain Valtz,[‡] Christophe Coquelet,[‡] Dominique Richon,[‡] Paramespri Naidoo,[†] and Deresh Ramjugernath*[,†]

Thermodynamics Research Unit, School of Chemical Engineering, University of KwaZulu-Natal, Durban 4041, South Africa, and MINES ParisTech, CEP/TEP Centre Énergétique et Procédés, 35 rue St Honoré, 77305 Fontainebleau Cedex, France

Experimental pure component vapor pressure data for hexafluoropropylene (R1216) and hexafluoropropylene oxide (HFPO) are presented. Experimental vapor−liquid equilibrium (VLE) data are presented at two temperatures, (273 and 313) K, for four binary systems: R1216 + toluene, HFPO + toluene, hexafluoroethane (R116) + R1216, and R116 + HFPO. The measurements were undertaken using both a "static−analytic" apparatus fitted with a pneumatic rapid online sampler injector (ROLSI) and a "static−synthetic" *PVT* apparatus. The experimental vapor pressure data were regressed to obtain correlated parameters for the Peng−Robinson (PR) and Soave−Redlich−Kwong (SRK) equations of state with the Mathias−Copeman α function. The binary VLE data were regressed to obtain correlated parameters for three different model combinations: the PR equation of state with the Wong−Sandler (WS) mixing rules, the PR equation of state with the modified Huron−Vidal first-order (MHV1) mixing rules, and the SRK equation of state with the WS mixing rules. The Mathias−Copeman α function and the nonrandom two-liquid (NRTL) excess Gibbs energy model were used in conjunction with the equations of state and mixing rules. In general, the PR equation of state with the WS mixing rules provided the best correlation for the experimental data. The critical lines for the supercritical systems R116 + R1216 and R116 + HFPO, calculated with the PR equation of state with the WS mixing rules, are also presented.

Introduction

The present work focuses on the measurement and modeling of thermodynamic data involving the fluorinated compounds hexafluoropropylene (R1216) and hexafluoropropylene oxide (HFPO). R1216 and HFPO are specialty fluorocarbons which have found extensive use in the fluorochemical industry. R1216 has gained prominence in both industrial and research activities and is utilized as an intermediate in chemical reactions,[1] as a monomer in fluoropolymers,[2,3] in etching applications,[4] and in epoxidation reactions for the manufacturing of HFPO.[5−7] The relatively more valuable commodity HFPO has found application in the manufacturing of high performance fluoropolymers and elastomers,[8] in the production of high performance lubricating oils and heat resistant fluids,[9] as a surfactant[10] in ion exchange membrane applications,[7] and in the manufacturing of rigid polyurethane foams.[11]

The advent of the Montreal Protocol[12] in 1987 led to the adoption of fluorocarbons and hydrofluorocarbons as alternatives to the environmentally harmful chlorofluorocarbons. Accurate experimental data are required to better understand and utilize these types of compounds in refrigeration processes or separation schemes. These data are of interest to evaluate the performance of refrigeration cycles, to determine the optimized composition of new refrigerant mixtures, or to investigate separation processes involving fluorinated compounds as either solutes or solvents. However, the measurement of vapor−liquid equilibrium (VLE) data is a necessary but not sufficient condition to accomplish these objectives. Coquelet and Richon[13] suggested that accurate experimental data *and* predictive techniques (via thermodynamic modeling of the VLE systems) are necessary to improve our understanding of the behavior and performance of these systems and processes.

The separation of R1216 and HFPO is difficult due to the proximity of the pure component boiling points ((243.75 and 245.75) K, respectively).[14] Extractive distillation processes for the separation of R1216 and HFPO have been patented for aromatic[15] chlorobenzene or chloroalkane[16,17] and hydrochlorofluorocarbon[18] solvents.

Although the use of toluene as an extractive solvent for this separation scheme has been patented by the DuPont company,[15] no experimental VLE data involving toluene and these compounds have previously been published. The thermodynamic data presented in this work can thus be used for the investigation of innovative separation processes for R1216 and HFPO utilizing perfluorocarbons such as R116, which can then be compared to a separation process involving known aromatic solvents such as toluene. The perfluoroalkane R116 is derived from ethane and utilized as an etching agent and refrigerant, while toluene is widely used as an industrial feedstock and solvent.

At present, there is a scarcity of published thermodynamic data for the fluorocarbons R1216 and HFPO. The Dortmund Data Bank[14] (DDB) contains five sets of pure component vapor pressure data for R1216, while no published pure component vapor pressure data for HFPO exist. In the case of binary VLE data, only five sets of data involving R1216 have been

* Corresponding author. E-mail: ramjuger@ukzn.ac.za. Telephone: +27 31 260 3128.
[†] University of KwaZulu-Natal.
[‡] MINES ParisTech, CEP/TEP.

10.1021/je900400v CCC: $40.75
Published on Web 10/27/2009

published,[19−22] while no published data for any binary VLE systems involving HFPO exist.

In this paper, experimental pure component vapor pressure data for R1216 and HFPO are presented in the temperature range of (272 K to 317) K and (271 K to 318) K, respectively. Experimental binary VLE data for the four systems, R1216 + toluene, R116 + R1216, HFPO + toluene, and R116 + HFPO, are presented at two temperatures, (273 and 313) K. The experimental data were measured at MINES ParisTech in Fontainebleau, France using two experimental techniques. The binary VLE data for the systems involving R1216, HFPO, and toluene were measured on a "static−synthetic" pressure−volume−temperature (*PVT*) apparatus. The pure component vapor pressure measurements and binary VLE for the systems involving R1216, HFPO, and R116 were measured on a "static−analytic" apparatus with a rapid online sampler injector[23] (ROLSI) and a gas chromatograph for equilibrium vapor and liquid phase sample handling and analysis.

All experimental data were modeled via the direct method in the computer software THERMOPACK[24] utilizing popular equation of state (EoS) models such as the Peng−Robinson[25] (PR) and Soave−Redlick−Kwong[26] (SRK) EoS in conjunction with the Mathias−Copeman[27] α function. For the data regression and modeling involving the PR EoS, two mixing rules were used to extend the EoS to mixtures, the Wong−Sandler[28] (WS) and modified Huron−Vidal first-order[29] (MHV1) mixing rules. For the data regression and modeling involving the SRK EoS, only the WS mixing rules were utilized. The excess Gibbs energy model incorporated into the WS and MHV1 mixing rules was the nonrandom two-liquid[30] (NRTL) activity coefficient model. The results for the data regression for the three model combinations, (1) PR EoS with the WS mixing rules, (2) PR EoS with the MHV1 mixing rules, and (3) SRK EoS with the WS mixing rules, are tabulated and reported in this work, while the thermodynamic modeling of the experimental data for the PR EoS and the WS mixing rules are presented graphically. The binary systems involving the component R116 reached the supercritical state at the 313 K isotherm. The critical lines for the supercritical systems R116 + R1216 and R116 + HFPO were calculated in THERMOPACK using the method of Stockfleth and Dohrn.[31]

Experimental Section

Materials. R1216 and HFPO were purchased in 500 g quantities from Interchim/Boc Edwards of Montluçon, France at specified minimum purities of 99.5 % and 99 %, respectively. Chromatography grade toluene was purchased from Prolabo/Merck, France at a minimum certified purity of 99.9 %. R116 was purchased from l′Air Liquide, France at a minimum certified purity of 99.999 %. All chemicals were degassed before use to remove any volatile impurities.

Apparatus and Experimental Procedures

"Static−Synthetic" PVT Apparatus. The binary VLE (*P*,*x* data sets) involving R1216, HFPO, and toluene were measured on a "static−synthetic" *PVT* apparatus similar to that described by Valtz et al.[32] For this method, no sampling of the equilibrium vapor and liquid phases was necessary, with the global composition of the mixture known beforehand via an accurate weighing procedure. The method was based on the use of a variable volume equilibrium cell which allowed the simultaneous determination of bubble pressures and saturated liquid molar volumes.

A membrane pressure transducer (Bourdon Sedeme, 250 bar maximum pressure) was fixed onto the cell for pressure measurements and calibrated against a dead-weight tester (Desgranges & Huot, model 5202S) with atmospheric pressure measured via a resonant sensor barometer (Druck, model DPI141). The pressure transducer was calibrated at the two temperatures of the measurements, namely, (273 and 313) K. Taking into account the uncertainties due to the calibrations, the resulting uncertainties on the pressure measurements for the *PVT* apparatus were estimated to be less than ± 0.005 MPa at 273 K and less than ± 0.004 MPa at 313 K. The equilibrium cell was housed in an air bath constructed by CLIMATS with a temperature operating range between (233 and 433) K and temperature regulation to within 0.1 K of set point as determined by the manufacturer. Three platinum resistance temperature probes (Pt 100) were located at different positions of the equilibrium cell and assembly, and the probes were connected to a digital read-out (FLUKE, model 2190A). The three probes were calibrated against a 25 Ω reference platinum resistance thermometer certified according to the ITS 1990 protocol.[33] Taking into account the uncertainties due to calibration, the resulting uncertainty on temperature measurements for the *PVT* apparatus was estimated to be less than ± 0.06 K.

The experimental procedure for the *PVT* apparatus was similar to that of Valtz et al.[32] The equilibrium cell was first removed from the air bath, cleaned with ethanol, evacuated, and weighed. The cell was light enough (1.8 kg) to allow the use of an accurate analytical balance of sensitivity of 10^{-6} kg (Mettler, model H305). After weighing the empty cell, the less volatile component was loaded. For the systems R1216 + toluene and HFPO + toluene, the toluene was injected via a plastic syringe directly into the loading line. The cell was degassed under vacuum and accurately weighed to precisely determine the amount of component added. For the addition of the light component, R1216, and in subsequent measurements of HFPO, the feed cylinder was heated to create a temperature gradient. After the addition of the light component, the cell was weighed and the global composition of the mixture calculated. The uncertainties on the liquid mole fraction (Δx) due to the weighing procedure were calculated and are tabulated with the experimental VLE data. The liquid mole fraction uncertainty is given by eq 1, with x_i as the liquid mole fraction of the components, Δm as the uncertainty due to the measurement of mass on the Mettler scale, m_i as the mass of the components, and M_i as the molar mass.

$$\Delta x_1 = x_1\left[\frac{\Delta m_1}{m_1} + \frac{\Delta m\left(\frac{1}{M_1} + \frac{1}{M_2}\right)}{\frac{m_1}{M_1} + \frac{m_2}{M_2}}\right] \quad (1)$$

The equilibrium cell was assembled in its housing, placed into the regulated air bath, and allowed to reach thermal equilibrium. Thermal equilibrium was assumed when the temperature probes gave equivalent equilibrium temperature values within their uncertainty values (± 0.06 K) for at least 10 min. The volume of the mixture within the equilibrium cell was varied through the displacement of a piston inside the cell and the mixture brought to the bubble point. A pressure versus volume curve for a specific composition of the binary mixture in the cell was obtained, and from the analysis of the break point on this curve the saturated pressure at a particular composition was evaluated. For several loadings at different compositions of a binary mixture, a *P*,*x* curve for the binary system was generated. Each loading of the equilibrium cell was

used to complete a measurement at (273 and 313) K; however, after each run for a particular composition, the cell had to be emptied and reloaded for the next composition. This was due to the degradation of the polymer o-rings caused by the components of the binary mixture which necessitated the replacement of the o-rings after each cell loading. In this manner large quantities of R1216 and HFPO were utilized for the measurements which made it possible to only measure four interior data points on the *P,x* envelope for the system R1216 + toluene and five interior data points for the system HFPO + toluene.

"Static−Analytic" Apparatus. The pure component vapor pressure measurements for R1216 and HFPO and the binary VLE (*P,x,y* data sets) involving R1216, HFPO, and R116 were measured on the "static−analytic" apparatus of Coquelet et al.[34] The analytical technique is classified as a direct sampling method with the composition of each equilibrium phase obtained through direct analysis of the sample via chromatographic techniques.

The equilibrium cell (titanium alloy, maximum internal volume of 50 cm^3) was immersed in a thermo-regulated liquid bath which utilized a temperature regulator for accurate control to within 0.1 K of set point as determined by the manufacturer. Internal stirring through the use of magnetic stirrers allowed the mixture to rapidly attain equilibrium. The temperature of the equilibrium cell was monitored via two platinum resistance (Pt 100) probes located inside wells drilled directly into the body of the cell. Pressure measurements were obtained via two pressure transducers (Druck, model PTX611) maintained at a constant temperature higher than the highest temperature of the measurements. The Pt 100 probes and pressure transducers were calibrated in a similar manner to the *PVT* apparatus, with resulting uncertainties on temperature and pressure measurements of ± 0.04 K and ± 0.0004 MPa (0 to 6 bar range) and 0.002 MPa (0 to 60 bar range), respectively. The temperature probes and pressure transducers were connected to an online data acquisition unit (HP, model 34970A), which was in turn connected to a personal computer via an RS-232 interface.

The equilibrium vapor and liquid samples obtained by the pneumatic ROLSI were analyzed in a gas chromatograph (VARIAN, model CP-3800) equipped with a thermal conductivity detector (TCD). The chromatograph utilized a PORAPAK N 80/100 mesh column of 3 m length and 3.2 mm diameter from Restek, France. An online data acquisition system (BORWIN, version 1.5) was utilized for the logging and analysis of the gas chromatographic data. The TCD was calibrated by repeated injections of a known quantity of each pure component into the gas chromatograph, and by noting the response of peak area to the amount of sample injected, calibration curves were generated. Taking into account the uncertainties due to the calibration and analyzing the deviation of the results, the resulting uncertainties on the vapor and liquid mole fractions were estimated to be less than ± 1 %.

The experimental procedure for the "static−analytic" apparatus was similar to that of Coquelet et al.[34] The equilibrium cell and the loading lines were first evacuated down to 10 Pa at room temperature. The equilibrium cell was first loaded with the less volatile liquid (approximately 5 cm^3 of R1216 or HFPO) and allowed to reach the equilibrium temperature of the measurement. Equilibrium was assumed when the two Pt 100 probes give equivalent equilibrium temperature values within their temperature uncertainty values (± 0.04 K) for at least 10 min. The pure component vapor pressure of the heavier component (R1216 or HFPO) at the equilibrium temperature was first recorded and the lighter or more volatile component then introduced into the equilibrium cell. The lighter component was introduced to obtain different compositions in a stepwise manner which led to successive equilibrium mixtures of increasing overall lighter component compositions. Each introduction of the lighter component to the cell corresponded to a single *PTxy* determination on the two-phase envelopes. Equilibrium was assumed when the total pressure remained unchanged within the pressure uncertainty values during a period of 10 min under efficient stirring. For each equilibrium condition, a minimum of five samples each of both the liquid and the vapor phases were withdrawn using the pneumatic ROLSI and analyzed to check for measurement reproducibility.

Table 1. Critical Property Parameters and Acentric Factors[35]

component	T_c / K	P_c / MPa	ω
R1216	368.12	2.902	0.204
HFPO	359.15[a]	2.926[b]	0.292[c]
toluene	591.7	4.114	0.257
hexafluoroethane	293.03	3.041	0.229

[a] Predicted using method detailed in ref 36. [b] Evaluated by fitting the experimental vapor pressure data to a polynomial equation and extrapolating to the critical temperature. [c] Acentric factor was determined from T_c, P_c, and P^{sat} values at $T_r = 0.7$.

Correlations. The pure component vapor pressure and binary VLE data were correlated in the noncommercial proprietary software THERMOPACK developed at the TEP laboratory in Fontainebleau.

The critical temperatures (T_c), critical pressures (P_c), and acentric factors (ω) for the components utilized for this work are provided in Table 1. The data for R1216, toluene, and R116 were obtained from the Component Plus[35] pure component database. The critical properties of HFPO were not available in either the Component Plus database or the DDB, and the required data were thus predicted. The critical temperature was evaluated using the method of Nannoolal et al.,[36] which required only the normal boiling point of the component of interest. The critical pressure was evaluated by fitting the experimental vapor pressure data to a polynomial equation and extrapolating to the critical temperature, while the acentric factor was determined from T_c, P_c, and P^{sat} values at $T_r = 0.7$.

To represent the pure component vapor pressures and the binary VLE data, the well-known PR (eq 2) and SRK EoS (eq 3) were utilized, where *a* is the EoS attractive parameter and *b* the EoS covolume parameter.

$$P = \frac{RT}{V-b} - \frac{a(T)}{V(V+b)+b(V-b)} \quad (2)$$

$$P = \frac{RT}{V-b} - \frac{a(T)}{V(V+b)} \quad (3)$$

To accurately represent the pure component vapor pressures of each component, the Mathias−Copeman α function with three adjustable parameters, c_1, c_2, and c_3, was utilized. Values for the α function parameters for the components used for this work are provided in Table 2. The parameters for toluene and R116 were obtained from the Component Plus database. The parameters for R1216 and HFPO were adjusted from the experimental pure component vapor pressure data over the entire temperature range of the measurements. A modified Simplex algorithm with the objective function given in eq 4 was utilized for both the PR and the SRK EoS for the parameter regression. *N* represents the number of data points, P_{exp} the measured pressure, and P_{cal} the calculated pressure.

Table 2. Mathias−Copeman Parameters for the PR EoS and SRK EoS[a]

	PR EoS			SRK EoS		
	c_1	c_2	c_3	c_1	c_2	c_3
R1216	−0.155	9.093	−26.212	−0.061	9.554	−28.264
HFPO	0.825	0.292	−2.757	0.928	−1.638	9.585
toluene	0.762	−0.042	0.271	0.925	−0.338	0.590
hexafluoroethane	0.646	0.984	−2.517	0.807	0.683	−2.171

[a] Toluene and R116 parameters from Component Plus,[35] R1216 and HFPO parameters regressed from experimental data.

Table 3. Experimental and Calculated Vapor Pressures for R1216 and HFPO ($\Delta P = P_{exp} - P_{cal}$)[a]

R1216				HFPO			
		PR EoS	SRK EoS			PR EoS	SRK EoS
T	P_{exp}	ΔP	ΔP	T	P_{exp}	ΔP	ΔP
K	MPa	MPa	MPa	K	MPa	MPa	MPa
272.33	0.3271	−0.0009	−0.0009	271.88	0.3022	0.0001	0.0001
279.64	0.4207	0.0020	0.0020	295.53	0.6499	−0.0019	−0.0019
299.34	0.7633	−0.0005	−0.0005	300.47	0.7456	0.0001	0.0002
302.24	0.8257	−0.0025	−0.0025	303.11	0.7985	0.0019	0.0019
312.33	1.0773	−0.0020	−0.0020	306.50	0.8747	0.0012	0.0012
317.63	1.2321	0.0045	0.0046	310.48	0.9701	0.0009	0.0009
				312.64	1.0249	−0.0012	−0.0012
				318.16	1.1753	−0.0013	−0.0014

[a] Calculated data via the PR and SRK EoS, with the Mathias−Copeman α function.

$$F = \frac{100}{N}\left[\sum\left(\frac{P_{exp} - P_{cal}}{P_{exp}}\right)^2\right] \quad (4)$$

Two mixing rules were used to extend the use of the PR and SRK EoS to mixtures, the MHV1[29] and WS[28] mixing rules. These mixing rules are both based on the MHV1[37] approach, which equates, at infinite pressure, the Gibbs energy calculated from the EOS and the Gibbs energy calculated from an activity coefficient model.

The excess Gibbs energy was calculated using the well-described NRTL[30] local composition model with adjustable parameters α_{ji}, τ_{ij}, and τ_{ji}. For polar systems, the value of α_{ji} is generally set to 0.3, while τ_{ij} and τ_{ji} are adjusted directly to VLE data through a modified simplex algorithm using an objective function.

For the data measured on the "static−analytic" apparatus, a flash adjustment was utilized and is given by eq 5.

$$F = \frac{1}{N}\left[\sum\left(\frac{x_{exp} - x_{cal}}{x_{exp}}\right)^2 + \sum\left(\frac{y_{exp} - y_{cal}}{y_{exp}}\right)^2\right] \quad (5)$$

For the data measured on the static synthetic *PVT* apparatus, a bubble-point adjustment on pressure was utilized and is given by eq 6.

$$F = \frac{1}{N}\left[\sum\left(\frac{P_{exp} - P_{cal}}{P_{exp}}\right)^2\right] \quad (6)$$

At the 313 K isotherm, the binary systems R116 + R1216 and R116 + HFPO entered the supercritical region. The calculation of the critical point and critical line were performed in THERMOPACK utilizing the algorithm of Stockfleth and Dohrn.[31] The algorithm was based on the works of Heidemann and Khalil[38] and Michelsen and Heidemann[39] which assumed that the stability criterion for an isothermal variation can be explained with a minimum of molar Helmholtz energy. Stockfleth and Dohrn improved on these works by developing a newer generalized algorithm which was used in conjunction with the PR EoS to calculate the critical lines for the supercritical systems at 313 K.

Table 4. VLE Pressures and Liquid Phase Compositions for R1216 (1) + Toluene (2) and HFPO (1) + Toluene (2) Mixtures at (273.15 and 313.15) K[a]

R1216 (1) + toluene (2)				HFPO (1) + toluene (2)			
T	P_{exp}			T	P_{exp}		
K	MPa	x_1	Δx_1	K	MPa	x_1	Δx_1
273.15	0.087	0.0854	0.0004	273.15	0.193	0.1765	0.0005
	0.166	0.2050	0.0004		0.197	0.2771	0.0004
	0.190	0.3909	0.0004		0.205	0.3722	0.0005
	0.186	0.7040	0.0006		0.201	0.7306	0.0006
313.15	0.349	0.0854	0.0004	313.15	0.797	0.1615	0.0005
	0.622	0.2050	0.0004		0.813	0.1765	0.0005
	0.747	0.3909	0.0004		0.816	0.2771	0.0004
	0.790	0.7040	0.0006		0.829	0.3722	0.0005
					0.809	0.7306	0.0006

[a] Liquid phase composition uncertainties (Δx_1) calculated by eq 1.

To quantify the fit of a model to the experimental data, the relative deviation (RD) in terms of the pressure and the liquid and vapor compositions was computed. Equation 7 defines the RD for pressure, vapor, and liquid mole fractions.

$$\mathrm{RD} - U = \frac{\left(\sum_{i=1}^{N}\left|\frac{U_i^{calc} - U_i^{exp}}{U_i^{exp}}\right|\right)}{N} \quad (7)$$

The BIAS of the measurements was calculated for the pressure, liquid, and vapor phase mole fractions and is given by eq 8.

$$\mathrm{BIAS} - U = \frac{\left(\sum_{i=1}^{N}\left(\frac{U_i^{calc} - U_i^{exp}}{U_i^{exp}}\right)\right)}{N} \quad (8)$$

N represents the number of data points, and U represents either P, x, or y. The BIAS can have either a positive or negative value; however, the better the fit of the data, the closer this value is to zero. The RD can only have a positive value because of the absolute value function and is a better indicator of the fit of the experimental and modeled data.

Table 5. VLE Pressures, Phase Compositions, and Standard Deviations on Composition Measurements (σx_1 and σy_1) for Hexafluoroethane (1) + R1216 (2) and Hexafluoroethane (1) + HFPO (2) Mixtures at (273.15 and 313.15) K

hexafluoroethane (1) + R1216 (2)						hexafluoroethane (1) + HFPO (2)					
T/K	P_{exp}/MPa	σx_1	x_1	σy_1	y_1	T/K	P_{exp}/MPa	σx_1	x_1	σy_1	y_1
273.15	0.5057	0.0008	0.1154	0.0006	0.3714	273.15	0.5314	0.0020	0.1562	0.0042	0.4516
	0.6935	0.0029	0.2463	0.0012	0.5790		0.7725	0.0020	0.3267	0.0004	0.6600
	1.0133	0.0030	0.4612	0.0010	0.7564		1.0371	0.0015	0.5111	0.0003	0.7878
	1.1863	0.0010	0.5884	0.0003	0.8243		1.1772	0.0005	0.6036	0.0010	0.8365
	1.4180	0.0004	0.7457	0.0011	0.8939		1.4015	0.0011	0.7422	0.0006	0.8987
	1.5402	0.0003	0.8218	0.0007	0.9253		1.6293	0.0009	0.8768	0.0012	0.9526
313.15	1.6760	0.0003	0.1454	0.0253	0.2537	313.15	1.6560	0.0005	0.1654	0.0036	0.2421
	2.0493	0.0006	0.2652	0.0020	0.4262		1.9984	0.0001	0.2690	0.0005	0.4452
	2.6021	0.0003	0.4367	0.0016	0.5667		2.5419	0.0011	0.4312	0.0006	0.5859
	2.9621	0.0002	0.5425	0.0005	0.6490		3.0224	0.0001	0.5696	0.0003	0.6580
	3.2983	0.0003	0.6437	0.0003	0.6864		3.3986	0.0006	0.6645		

Table 6. Fitted Model Parameters for the R1216 (1) + Toluene (2) and HFPO (1) + Toluene (2) Systems at (273.15 and 313.15) K

	R1216 (1) + toluene (2)				HFPO (1) + toluene (2)			
model	T/K	$k_{1,2}$	$\tau_{1,2}$/J·mol^{-1}	$\tau_{2,1}$/J·mol^{-1}	T/K	$k_{1,2}$	$\tau_{1,2}$/J·mol^{-1}	$\tau_{2,1}$/J·mol^{-1}
PR−WS	273.15	−0.7720	5850.0	4150.0	273.15	−0.5087	5299.6	5924.0
	313.15	−0.2561	7224.0	2961.1	313.15	0.0644	3656.5	5013.3
PR−MHV1	273.15		−837.0	4456.3	273.15		133.4	6136.5
	313.15		1228.8	3224.8	313.15		2068.6	5194.7
SRK−WS	273.15	−0.7627	5948.8	4081.8	273.15	−0.3873	5411.6	5579.0
	313.15	−0.2510	7444.2	2896.1	313.15	0.0750	4505.5	4992.3

Table 7. RD and BIAS Values for the R1216 (1) + Toluene (2) and HFPO (1) + Toluene (2) Systems at (273.15 and 313.15) K

	R1216 (1) + toluene (2)				HFPO (1) + toluene (2)			
	T = 273.15 K		T = 313.15 K		T = 273.15 K		T = 313.15 K	
model	RD P/%	BIAS P/%	RD P/%	BIAS P/%	RD P/%	BIAS P/%	RD P/%	BIAS P/%
PR−WS	5.06	0.49	0.9	0.17	1.01	0.54	0.7	0.01
PR−MHV1	6.67	3.03	3.08	1.27	3.39	0.84	0.72	0.01
SRK−WS	5.13	0.51	1.06	0.21	5.07	−1.64	2.92	1.18

Table 8. Fitted Model Parameters for the Hexafluoroethane (1) + R1216 (2) and Hexafluoroethane (1) + HFPO (2) Systems at (273.15 and 313.15) K

	hexafluoroethane (1) + R1216 (2)				hexafluoroethane (1) + HFPO (2)			
model	T/K	$k_{1,2}$	$\tau_{1,2}$/J·mol^{-1}	$\tau_{2,1}$/J·mol^{-1}	T/K	$k_{1,2}$	$\tau_{1,2}$/J·mol^{-1}	$\tau_{2,1}$/J·mol^{-1}
PR−WS	273.15	−0.0027	1451.9	−548.4	273.15	−0.0377	3179.6	−1721.9
	313.15	0.1444	−2295.3	3509.2	313.15	0.0677	6631.6	−3000.3
PR−MHV1	273.15		−529.9	729.4	273.15		529.3	−551.4
	313.15		2071.1	−1238.2	313.15		3712.6	−2259.8
SRK−WS	273.15	−0.0168	2105.1	−882.4	273.15	0.0509	−721.7	292.6
	313.15	0.1413	306.9	−0.1	313.15	0.1067	1350.8	−1289.6

Table 9. RD and BIAS Values for the Hexafluoroethane (1) + R1216 (2) and Hexafluoroethane (1) + HFPO (2) Systems at (273.15 and 313.15) K

		hexafluoroethane (1) + R1216 (2)				hexafluoroethane (1) + HFPO (2)			
	model	RD x_1/%	RD y_1/%	BIAS x_1/%	BIAS y_1/%	RD x_1/%	RD y_1/%	BIAS x_1/%	BIAS y_1/%
T = 273.15 K	PR−WS	1.4	0.8	0.9	−0.7	0.7	0.8	−0.1	0.6
	PR−MHV1	1.1	0.8	−0.1	−0.4	0.9	0.9	0.7	0.3
	SRK−WS	1.3	0.8	0.8	−0.6	1.3	2.7	0.6	2.3
T = 313.15 K	PR−WS	1.7	2.9	−0.2	2.7	1.3	4.1	−1.3	4.1
	PR−MHV1	2.1	3.6	−0.7	1.4	1.7	4.3	−1.1	4.1
	SRK−WS	1.8	3.5	−0.3	3.3	4.1	6.1	−3.3	4.6

A small BIAS and a large RD usually indicates a systematic deviation between the experimental and the predicted data.

Results and Discussion

Vapor Pressures. The experimental pure component vapor pressure data for R1216 and HFPO are presented in Table 3. Both sets of measured data were correlated with the PR and SRK EoS and the differences between the experimental and calculated pressures evaluated. The ΔP values in Table 3 show a good agreement between the experimental and the correlated data. The Mathias−Copeman coefficients (c_1, c_2, and c_3) adjusted from the experimental data are presented in Table 2 for both the PR and the SRK EoS.

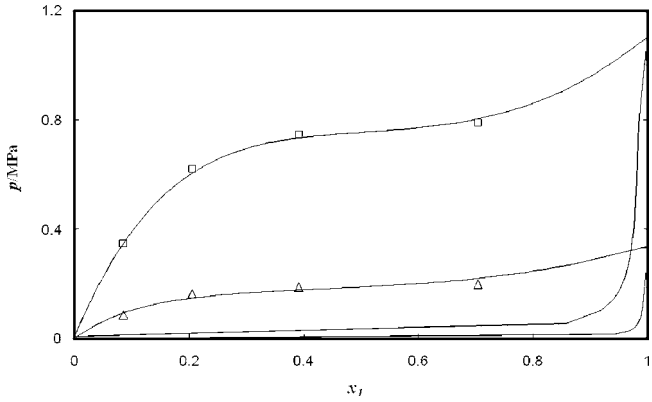

Figure 1. VLE data for the system R1216 (1) + toluene (2). Δ, 273.15 K; □, 313.15 K; solid line, modeled data calculated with the PR EoS, WS mixing rules, and NRTL model.

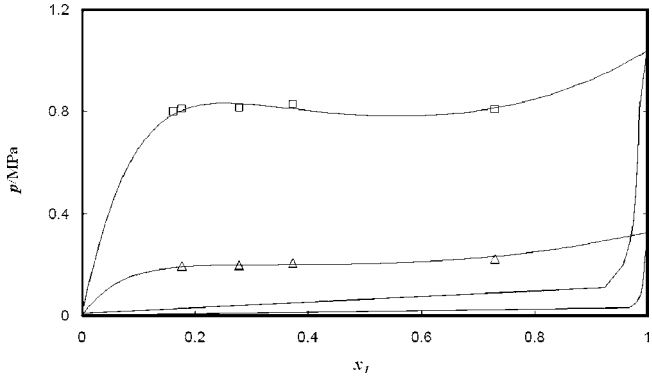

Figure 2. VLE data for the system HFPO (1) + toluene (2). Δ, 273.15 K; □, 313.15 K; solid line, modeled data calculated with the PR EoS, WS mixing rules, and NRTL model.

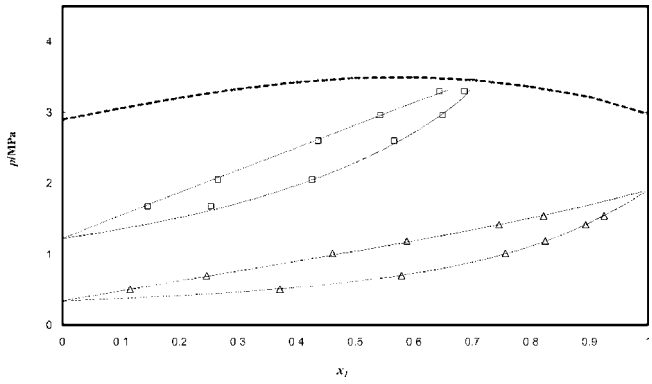

Figure 3. VLE data for the system hexafluoroethane (1) + R1216 (2). Δ, 273.15 K; □, 313.15 K; solid line, modeled data calculated with the PR EoS, WS mixing rules, and NRTL model; dashed line, critical locus calculated with the PR EoS, WS mixing rules, and NRTL model.

VLE Data. The experimental data for the binary systems R1216 + toluene and HFPO + toluene are presented in Table 4. The uncertainties of the liquid phase mole fractions are determined by eq 1 and are tabulated with the experimental data. The low uncertainty values reported for both of the systems involving toluene ($x_1 < 0.0006$) are indicative of the accuracy of the weighing procedure and experimental measurements on the *PVT* apparatus.

The experimental data for the binary systems R116 + R1216, and R116 + HFPO are presented in Table 5. The standard deviations of the liquid and vapor sample measurements are also provided in Table 5. The reported low deviations for both

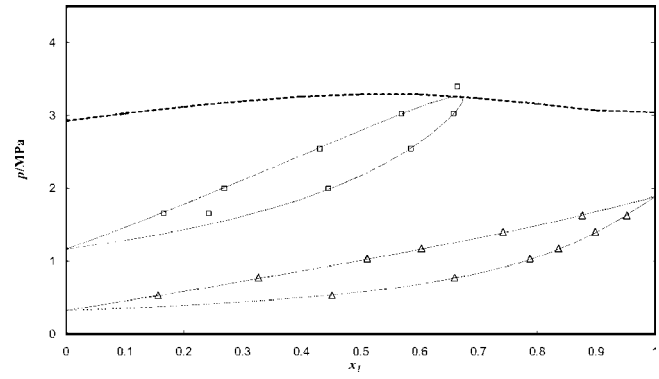

Figure 4. VLE data for the system hexafluoroethane (1) + HFPO (2). Δ, 273.15 K; □, 313.15 K; solid line, modeled data calculated with the PR EoS, WS mixing rules, and NRTL model; dashed line, critical locus calculated with the PR EoS, WS mixing rules, and NRTL model.

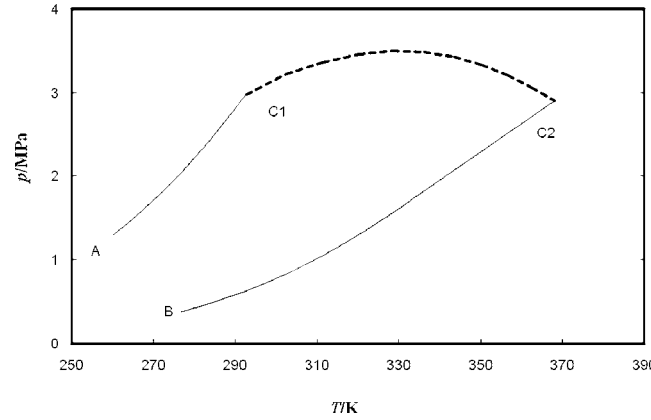

Figure 5. *PT* diagram for the system hexafluoroethane (1) + R1216 (2). Dashed line, critical locus calculated with the PR EoS, WS mixing rules, and NRTL model. Curve A−C1 (hexafluoroethane pure component vapor pressure) and curve B−C2 (R1216 pure component vapor pressure) are calculated with the PR EoS and Mathias−Copeman α function.

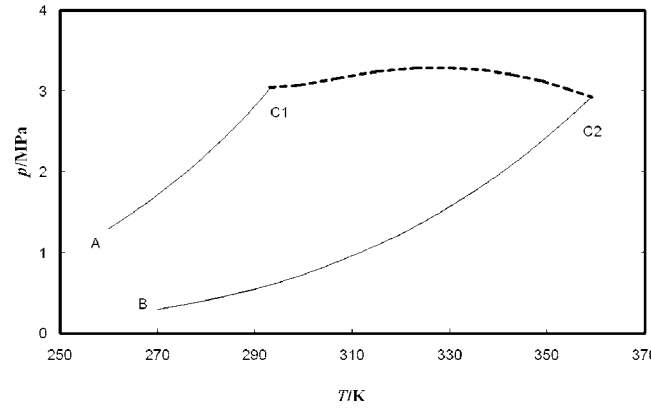

Figure 6. *PT* diagram for the system hexafluoroethane (1) + HFPO (2). Dashed line, critical locus calculated with the PR EoS, WS mixing rules, and NRTL model. Curve A−C1 (hexafluoroethane pure component vapor pressure) and curve B−C2 (the HFPO pure component vapor pressure) are calculated with the PR EoS and Mathias−Copeman α function.

systems measured on the static−analytic apparatus and ROLSI are indicative of the reproducibility and precision of the measurements. For the system R116 + HFPO at the 313 K isotherm, a single data point at the equilibrium pressure of 3.3986 MPa was measured in the supercritical region.

Modeling. Three thermodynamic model combinations were used to regress and model the experimental VLE data: (1) PR EoS with the WS mixing rules, (2) PR EoS with the MHV1

Table 10. Critical Locus Data for the Hexafluoroethane (1) + R1216 (2) and Hexafluoroethane (1) + HFPO (2) Systems Calculated with the PR EoS, WS Mixing Rules, and the NRTL Activity Coefficient Model

hexafluoroethane (1) + R1216 (2)			hexafluoroethane (1) + HFPO (2)		
	P_{cal}	T_{cal}		P_{cal}	T_{cal}
x_1	MPa	K	x_1	MPa	K
0.0	2.9000	368.00	0.0	2.9260	359.15
0.1	3.0611	362.54	0.1	3.0300	354.00
0.2	3.2073	356.69	0.2	3.1200	349.00
0.3	3.3323	350.38	0.3	3.2000	343.00
0.4	3.4285	343.61	0.4	3.2600	337.00
0.5	3.4871	336.33	0.5	3.2900	330.00
0.6	3.4996	328.54	0.6	3.2900	323.00
0.7	3.4593	320.25	0.7	3.2400	315.00
0.8	3.3644	311.52	0.8	3.1600	307.00
0.9	3.2209	302.42	0.9	3.0700	299.00
1.0	2.9800	292.80	1.0	3.0410	293.04

mixing rules, and (3) SRK EoS with the WS mixing rules. All three combinations utilized the Mathias−Copeman α function and NRTL excess Gibbs energy model.

A bubble-point adjustment on pressure, eq 6, was used for the systems R1216 + toluene and HFPO + toluene. The model parameters (k_{ij}, τ_{ji}, and τ_{ij}) are presented in Table 6. To quantify the fit of the experimental data, the RD *P* and BIAS *P* values were calculated and are provided in Table 7. A flash adjustment, eq 5, was used for the systems R116 + R1216 and R116 + HFPO. The model parameters (k_{ij}, τ_{ji}, and τ_{ij}) are presented in Table 8. The RD x_1, RD y_1, BIAS x_1, and BIAS y_1 values were calculated and are provided in Table 9.

The VLE data for the four binary systems are presented graphically in Figures 1, 2, 3, and 4. The experimental data and the corresponding data modeled by the PR−WS model set at each temperature of measurement are graphed. The critical loci for the systems R116 + R1216 and R116 + HFPO were calculated in THERMOPACK using the experimental data in conjunction with the PR EoS, WS mixing rules, and NRTL activity coefficient model. The data is presented numerically in Table 10, while the critical loci for the supercritical systems are superimposed onto the VLE graphs in Figures 3 and 4 for the respective systems. Figures 5 and 6 present the respective *P*,*T* diagrams for the systems R116 + R1216 and R116 + HFPO, with the pure component vapor pressure curves predicted from the Mathias−Copeman parameters and the PR EoS, with the critical loci calculated as before.

Conclusions

In this paper, experimental data for the two fluorocarbons, R1216 and HFPO, with two solvents, toluene and R116, are presented. The measurements were performed on a "static−analytic" apparatus fitted with a pneumatic ROLSI and a "static−synthetic" *PVT* apparatus. Experimental pure component vapor pressure data for R1216 and HFPO and experimental VLE data, at (273 and 313) K, are presented for four binary systems: R1216 + toluene, HFPO + toluene, R116 + R1216, and R116 + HFPO. The four binary systems and pure component vapor pressure data for HFPO have not been previously reported in literature. The experimental vapor pressure data were fitted to the PR and SRK EoS, and adjusted Mathias−Copeman α function parameters were obtained. The binary VLE data were fitted to three different model combinations, and the mixing rule interaction parameter (k_{ij}) and NRTL binary interaction parameters (τ_{ij} and τ_{ji}) were obtained. In general, the PR EoS with the WS mixing rules correlated the experimental data the best. The critical lines for the supercritical systems R116 + R1216 and R116 + HFPO, calculated with the PR EoS and WS mixing rules and the experimental data, are also presented.

Literature Cited

(1) Krespan, C. G. Fluoroalkyl Azide Chemistry. *J. Org. Chem.* **1986**, *51*, 332–337.

(2) Aravindan, V.; Vickraman, P. Polyvinylidenefluoride-hexafluoropropylene based nanocomposite polymer electrolytes (NCPE) complexed with $LiPF_3(CF_3CF_2)_3$. *Eur. Polym. J.* **2007**, *43*, 5121–5127.

(3) Stolarska, M.; Niedzicki, L.; Borkowska, R.; Zalewska, A.; Wieczorek, W. Structure, transport properties and interfacial stability of PVdF/HFP electrolytes containing modified inorganic filler. *Electrochim. Acta* **2007**, *53*, 1512–1517.

(4) Bian, J. F.; Lujan, W. R.; Harper-Nixon, D.; Jeon, H. S.; Weinkauf, D. H. Effect of hexafluoropropylene oxide plasma polymer particle coatings on the rheological properties of boron nitride/poly(dimethylsiloxane) composites. *J. Colloid Interface Sci.* **2005**, *290*, 582–591.

(5) Atkins, G. M. Process for the epoxidation of Hexafluoropropylene. U.S. Patent 3775439, E. I. du Pont de Nemours and Company, 1973.

(6) Huang, Z.; Zhang, Y.; Zhao, C.; Qin, J.; Li, H.; Xue, M.; Liu, Y. Direct gas-phase epoxidation of hexafluoropropylene with molecular oxygen using Ag catalyst. *Appl. Catal., A* **2006**, *303*, 18–22.

(7) Ikeda, M.; Miura, M.; Aoshima, A. Process for the production of hexafluoropropylene oxide. U.S. Patent 4902810, Asahi Kogaku Kogyo Kabushiki Kaisha, 1990.

(8) Hirao, A.; Sugiyama, K.; Yokoyama, H. Precise synthesis and surface structures of architectural per- and semifluorinated polymers with well-defined structures. *Prog. Polym. Sci.* **2007**, *32*, 1393–1438.

(9) Ohsaka, Y.; Tohzuka, T. Process for preparing hexafluoropropene oxide. U.S. Patent 4288376, Daikin Kogyo Company Limited, 1981.

(10) Darling, T. R. Purification and polymerization of hexafluoropropylene oxide. U.S. Patent 4356291, E. I. du Pont de Nemours and Company, 1982.

(11) Shibanuma, T.; Tsuchiya, T.; Yamada, Y.; Shibata, N. Process for producing synthetic resin foam. U.S. Patent Application 10/493215, Settsu-shi, 2005.

(12) *Montreal Protocol on substances that deplete the ozone layer*; United Nations Environmental Program (UNEP): New York, 1987.

(13) Coquelet, C.; Richon, D. Need of thermodynamic properties: Measurements and modeling in the frame of new regulations on refrigerants. *J. Zheijiang Univ., Sci. A* **2007**, *8*, 724–733.

(14) *Dortmund Data Bank Software and Separation Technology*; DDBST GmbH: Oldenburg, Germany, 2007.

(15) Wiist, H. A. *Extractive distillation of hexafluoropropylene epoxide mixture - Patent 3326780*. E. I. du Pont de Nemours and Company, Patent, U. S., 1967.

(16) Sulzbach, R. Process for the preparation of pure Hexafluoropropylene Oxide. U.S. Patent 4358348, Hoechst Aktiengesellschaft, 1982.

(17) Oda, Y.; Uchida, K.; Morikawa, S. Method of Purifying Hexafluoropropylene Oxide. U.S. Patent 4134796, Asahi Glass Company Limited, 1979.

(18) Ueno, T.; Tatematsu, S.; Sato, M.; Ehata, K. Separation of Hexafluoropropylene Oxide and Hexafluoropropylene by solvent extraction and distillation. Japanese Patent 09020765, Asahi Glass Company Limited, 1997.

(19) Chen, Z.; Feng, Y.; Yaosheng, W.; Zhaoli, T. Isobaric vapor-liquid equilibria of the binary system of octafluorocyclobutane with dichlorodifluoromethane, chlorodifluoromethane and hexafluoropropylene. *Huagong Xuebao (Chin. Ed.)* **1989**, *40*, 113–117.

(20) Ho, Q. N.; Lee, B. G.; Kim, H. G.; Lim, J. S. Vapor-liquid equilibria for the binary mixture of octafluoropropane + hexafluoropropylene. In *Frontiers on Separation Science and Technology*, Proceedings of the International Conference on Separation Science and Technology, 4th, Nanning, China, Feb. 18−21, 2004; Vol. 1, pp 136−141.

(21) Maletskii, V. Y.; Kogan, V. B. Liquid-vapor equilibrium in binary systems formed by difluorochloromethane, hexafluoropropylene, and trifluorochloroethylene. *Russ. Chem. Rev.* **1966**, *42*, 626–628.

(22) Whipple, G. H. Vapor-Liquid Equilibria of Some Fluorinated Hydrocarbon Systems. *Ind. Eng. Chem.* **1952**, *44*, 1664–1667.

(23) Guilbot, P.; Valtz, A.; Legendre, H.; Richon, D. Rapid on-line sampler-injector: a reliable tool for HT-HP sampling and on-line GC analysis. *Analusis* **2000**, *28*, 426–431.

(24) Coquelet, C.; Baba-Ahmed, A. *ThermoPack*, version 1.10; Ecole des Mines de Paris, Laboratory of Thermodynamics and Phase Equilibria: Paris, 2002.

(25) Peng, D.; Robinson, D. B. A new two-constant equation of state. *Ind. Eng. Chem. Fundam.* **1976**, *15*, 59–64.

(26) Soave, G. Equilibrium constants for modified Redlich-Kwong equation of state. *Chem. Eng. Sci.* **1972**, *27*, 1197–1203.

(27) Mathias, P. M.; Copeman, T. W. Extension of the Peng-Robinson Equation of State to Complex Mixtures: Evaluation of Various Forms of the Local Composition Concept. *Fluid Phase Equilib.* **1983**, *13*, 91–108.
(28) Wong, D. S. H.; Sandler, S. I. A theoretically correct mixing rule for cubic equations of state. *AIChE J.* **1992**, *38*, 671–680.
(29) Michelsen, M. L. A modified Huron-Vidal mixing rule for cubic equations of state. *Fluid Phase Equilib.* **1990**, *60*, 213–219.
(30) Renon, H.; Prausnitz, J. M. Local Composition in Thermodynamic Excess Function for Liquid Mixtures. *AIChE J.* **1968**, *14*, 135–144.
(31) Stockfleth, R.; Dohrn, R. An algorithm for calculating critical points in multicomponent mixtures which can easily be implemented in existing programs to calculate phase equilibria. *Fluid Phase Equilib.* **1998**, *145*, 43–52.
(32) Valtz, A.; Laugier, S.; Richon, D. Bubble pressures and saturated liquid molar volumes of difluoromonochloromethane-fluorochloroethane binary mixtures: experimental data and modelling. *Int. J. Refrig.* **1986**, *9*, 282–289.
(33) BIPM Bureau International des Poids et Mesures, ITS-90 Documents. http://www.bipm.org/en/publications/its-90.html (accessed January 15, 2009).
(34) Coquelet, C.; Nguyen Hong, D.; Chareton, A.; Baba-Ahmed, A.; Richon, D. Vapour-liquid equilibrium data for the difluoromethane + 1,1,1,2,3,3,3- heptafluoropropane system at temperatures from 283.20 to 343.38 K and pressures up to 4.5 MPa. *Int. J. Refrig.* **2003**, *26*, 559–565.
(35) ProSim Component Plus 3.00; ProSim SA: Labege Cedex, France, 2001.
(36) Nannoolal, Y.; Rarey, J.; Ramjugernath, D. Estimation of pure component properties: Part 2. Estimation of critical property data by group contribution. *Fluid Phase Equilib.* **2007**, *252*, 1–27.
(37) Huron, M. J.; Vidal, J. New Mixing Rules in Simple Equations of State for Representing Vapour-Liquid Equilibria of Strongly non-ideal Mixtures. *Fluid Phase Equilib.* **1979**, *3*, 255–271.
(38) Heidemann, R. A.; Khalil, A. M. The Calculation of Critical Points. *AIChE J.* **1980**, *26*, 769–779.
(39) Michelsen, M. L.; Heidemann, R. A. Calculation of critical points from cubic 2 constant equations of state. *AIChE J.* **1981**, *27*, 521–523.

Received for review May 5, 2009. Accepted October 5, 2009. We thank the National Research Foundation (NRF) International Science Liaison and the Nuclear Energy Corporation of South Africa (NECSA) for financial support, as well as Albert Chareton for help in using the *PVT* apparatus. This work is based upon research supported by the South African Research Chairs Initiative of the Department of Science and Technology, National Research Foundation, and CNRS.

JE900400V